Correlation between non-Fermi-liquid behavior and antiferromagnetic fluctuations in $(TMTSF)_2PF_6$ observed using ^{13}C-NMR spectroscopy

Yoshitaka Kimura, Masaki Misawa, and Atsushi Kawamoto*
Department of Condensed Matter Physics, Hokkaido University, Kita-ku, Sapporo, Hokkaido 060-0810, Japan
(Received 7 June 2011; published 18 July 2011)

In the temperature-pressure phase diagram of the organic superconductor $(TMTSF)_2PF_6$ (TMTSF: tetramethyltetraselenafulvalene), the superconducting phase and the spin-density-wave (SDW) phase are adjacent to each other. This salt exhibits non-Fermi-liquid (NFL) behavior and superconductivity under pressure. Its superconductive property does not exist at higher pressures where Fermi-liquid (FL) behavior is exhibited. In order to investigate the origin of NFL behavior, systematic ^{13}C-NMR measurement of this salt has been assessed under pressure in a wide temperature range. At low temperatures, $(T_1T)^{-1}$ increases, and this increase is suppressed by the increasing pressure. These results suggest that applying pressure alters the electron system from the NFL to the FL state, and that antiferromagnetic fluctuations contribute to the origin of NFL behavior. The connection between the emergence of FL behavior and the disappearance of superconductivity suggests that the SDW fluctuation relates to the mechanism of the superconductivity in $(TMTSF)_2PF_6$.

DOI: 10.1103/PhysRevB.84.045123 PACS number(s): 71.30.+h, 74.70.Kn, 76.60.−k

I. INTRODUCTION

The phase diagrams of organic superconductors are similar to those of strongly correlated electron systems such as high-T_c cuprate and heavy-fermion superconductors.[1] The superconducting and the antiferromagnetic phases are in close proximity in the temperature-pressure or temperature-doping phase diagram, which indicates correlations between the antiferromagnetic fluctuations and the superconductivity. $(TMTSF)_2X$ (TMTSF: tetramethyltetraselenafulvalene) is a quasi-one-dimensional organic conductor, where X^- is a monovalent anion which exhibits various phases with changes in temperature, pressure, and X^-. These salts are called Bechgaard salts because they were first synthesized by Bechgaard *et al.*[2] The conducting chains of organic molecules exhibit high conductivity along the *a* axis.[3] The Bechgaard salt $(TMTSF)_2PF_6$ exhibits a spin-density-wave (SDW) phase and a superconducting phase in close proximity with the temperature-pressure phase diagram, as shown in Fig. 1.[4]

Doiron-Leyraud *et al.* measured the *a* axis electrical resistivity of $(TMTSF)_2PF_6$ at low temperatures as a function of pressure.[5] On the verge of the SDW order (1.18 GPa), where T_{SDW} decreases to 0 K, the superconducting transition temperature T_c reaches a maximum, and the resistivity shows linear temperature dependence. As pressure is increased, T_c decreases. At 2.08 GPa, the superconductivity ceases to exist and the resistivity shows T^2 dependence, which is characteristic of Fermi-liquid (FL) behavior. These results suggest a connection between the scattering mechanism of non-Fermi-liquid (NFL) behavior and superconductivity.

Considering that the SDW and superconducting phases are adjacent, antiferromagnetic fluctuation of the SDW is expected to be the origin of NFL behavior.[6,7] In order to examine the origin of NFL behavior, nuclear magnetic resonance (NMR) measurements are one of the best tools available. This technique has several advantages over others, including its ability to measure the uniform spin susceptibility under pressures such as the Knight shift and to observe magnetic fluctuations from the spin-lattice relaxation time T_1. There have been many NMR studies of ^1H and ^{77}Se nuclei in $(TMTSF)_2PF_6$.[8–10] Because phase separation is expected to occur near the phase boundary, multisite NMR such as ^1H or ^{77}Se involves an experimental ambiguity arising from the superposition of the multisite spectra. Moreover, if a spatial inhomogeneity occurs, the mixing of the fast relaxation from the SDW phase and the slow relaxation from the metallic phase modulates the relaxation profile of T_1. To verify the spatial inhomogeneity experimentally, single-site ^{13}C-NMR is desired. In the conventional composition method, both sides of the C=C bond in the TSF molecular frame are replaced with ^{13}C. With this enrichment, spectral splitting occurs because of the resulting coupled spin system and induces a so-called *Pake doublet*.[11] The two intrinsic peaks split into four peaks with J modulation, which inhibits the refocusing of the spin-echo signal. The mixing of the spin states also modifies the relaxation profile. Single-site ^{13}C enrichment, as shown in Fig. 1, suppresses the formation of the coupled spin system and enables the site-selective measurement of the ideal $I = 1/2$ spin system. Using this single-site ^{13}C enrichment, we can verify the spatial inhomogeneity from the spectra and relaxation profiles and measure the ideal T_1. The ^{13}C-NMR spectrum of $(TMTSF)_2PF_6$ with a 10% enrichment of ^{13}C isotopes at the central C=C sites was only reported at low temperatures.[12] In previous ^{13}C-NMR spectra of organic conductors, the quantitative analysis was hindered by the presence of the *Pake doublet* or by low signal intensity. Moreover, no systematic work has been conducted at pressures above 1.1 GPa, corresponding to the work of Doiron-Leyraud *et al.* Hence, the systematic measurement of T_1 and the Knight shift under high pressures over a wide temperature range is desired. To obtain an adequate signal-to-noise ratio at high temperatures, a TMTSF molecule with 100% enrichment of ^{13}C isotopes on only one side of the central carbon sites is required. Therefore, by using $(TMTSF)_2PF_6$, which was synthesized by the enriched method, we employed ^{13}C-NMR to assess the electronic state of this salt at ambient pressure and under other pressures over a wide temperature range

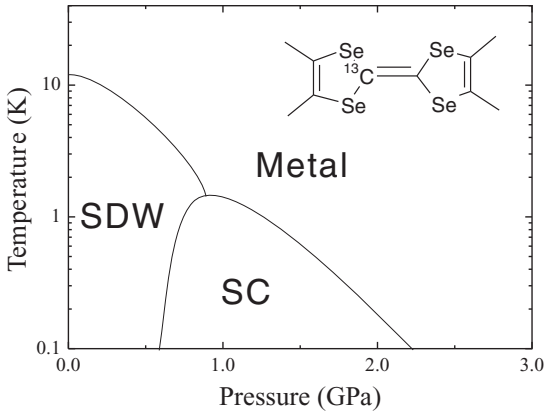

FIG. 1. Temperature-pressure phase diagram of $(TMTSF)_2PF_6$ (Ref. 4).

and investigated the magnetic fluctuations and their pressure dependence.

II. EXPERIMENT

A. The sample preparation

The isotope-enriched molecule was synthesized from the coupling of the tin complex. Because the well-established synthetic route to prepare TMTSF[13,14] is not suitable for isotope substitution, we explored an alternative route. The single-site ^{13}C-enriched molecule is an unsymmetrical donor. Among the synthetic routes to prepare unsymmetrical donors, those used to prepare symmetrical donors, which can be optimized by other elegant routes, have not yet been considered, but may be worthy of doing so. Figure 2 shows one such candidate, the synthetic route of Yamada *et al.* using dibutyltin complex.[15] Advantages of this method are that the isotope reagent dichloroacetic acid methyl ester is available and that Yamada *et al.* have already established the precursors of **4** and **5**. We synthesized single-site ^{13}C-enriched TMTSF by Yamada's method and characterized the products by mass spectroscopy and ^{1}H-NMR. The method enables the preparation of enriched radical salts using a conventional electrochemical cell, and may be useful for preparing other enriched donor molecules as well. The single crystal was prepared electrochemically.

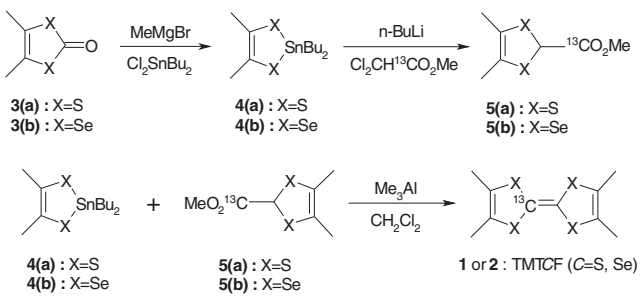

FIG. 2. Synthetic route to prepare single-site ^{13}C-enriched TMT*C*F.

B. The NMR spectroscopy

Temperature-dependent ^{13}C-NMR measurements were performed at decreasing temperatures under a magnetic field of 9.4 T, and the spectra were obtained by fast Fourier transformation of an echo signal with a $\pi/2$-π pulse sequence with a typical $\pi/2$ pulse width of 4 μs. The NMR shift is measured with reference to tetramethylsilane. Spin-lattice relaxation time was determined by the saturation recovery method. ^{13}C-NMR was performed under ambient pressure and at 0.8, 1.0, 1.4, and 1.8 GPa by using a clamp cell made of a NiCrAl alloy that can withstand a maximum pressure of 2.0 GPa at low temperatures. Daphni oil 7373 was used as the pressure medium. We corrected pressures using the resistivity of a wire made from lead at low temperatures. The additional magnetic field intensity from the pressure cell was corrected using the temperature dependence of the NMR shift with and without the cell. ^{13}C-NMR was performed with the external field applied along the b' axis to suppress the field-induced SDW.[16] The static susceptibility was measured using polycrystals by using a commercially available superconducting quantum interference device (SQUID) magnetometer.

III. DISCUSSION OF RESULTS

A. Hyperfine coupling tensors and chemical shift

Figure 3(a) displays the NMR spectra at 100 K and the lowest temperature 3 K at 0.8 GPa. The two peaks (denoted by H and L) in the metallic state correspond to two crystallographic-independent ^{13}C sites.[3] While we observed the SDW spectrum below 11.5 K under ambient pressure, we observed only the metallic state spectra down to 3 K under a pressure of 0.8 GPa without any significant broadening or splitting because of the emergence of the SDW phase.

In order to reveal the temperature dependence of the Knight shift K, we estimated the chemical shift σ. The NMR shift δ is expressed by $K + \sigma = A\chi_s(T) + \sigma$, where A and χ_s are the hyperfine-coupling constant (HFCC) and the uniform spin susceptibility, respectively. The uniform spin susceptibility is also expressed as $\chi_s(T) = \chi_T(T) - \chi_{\rm dia}$. Here, $\chi_T(T)$ and $\chi_{\rm dia}$ are the static susceptibility and the temperature-independent diamagnetic term of the orbital, respectively. Because the uniform spin susceptibility is proportional to K, it can be

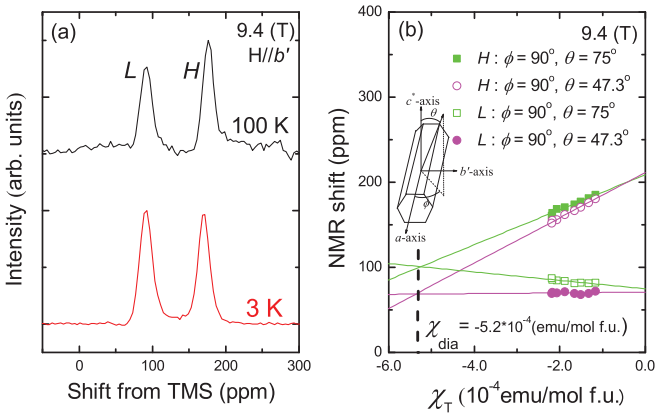

FIG. 3. (Color online) (a) NMR spectra under 0.8 GPa at 100 and 3 K. (b) χ_T-δ plot at ambient pressure.

TABLE I. A and σ at various angles.

θ	ϕ	A_H (kOe/μ_B)	A_L (kOe/μ_B)	σ (ppm)
−15°	90°	1.31	−0.11	99.85
12.7°	90°	1.46	0.20	71.18
47.3°	90°	1.49	0.02	71.53
75°	90°	1.19	−0.28	100.22
0°	136°	1.19	−0.26	99.55
30°	136°	2.29	0.61	59.92
45°	136°	3.14	1.01	50.94
60°	136°	4.30	1.80	23.05
90°	136°	5.17	2.28	22.99
90°	180°	8.95	5.02	−76.53

measured under pressures as K. The estimation of K depends on σ; therefore, we estimated σ from the χ_T-δ plot. The χ_T-δ plot with several angles at ambient pressure is shown in Fig. 3(b). From previous formulas, we derived the relational expression $\delta_i = A_i \{\chi_T(T) - \chi_{\rm dia}\} + \sigma$, where i denotes the crystallographic-independent site H or L. The HFCC depends on the crystallographic position, whereas σ depends only on the site position in a molecule.[17,18] Hence, the intersection point of the two lines of $i = L$ and $i = H$ represents ($\chi_{\rm dia}$,σ). As shown in Fig. 3(b), $\chi_{\rm dia}$ has almost the same values of -5.2×10^{-4} (emu/mol f.u.), and σ along the b' axis is estimated as 118(5) ppm. The value of $\chi_{\rm dia}$ is consistent with the previous estimation by Scott *et al.*[19] Constants A and σ are expressed by the hyperfine-coupling tensor $\overleftrightarrow{A}$ and the chemical-shift tensor $\overleftrightarrow{\sigma}$ caused by molecular anisotropy according to the relationships $A = \tilde{\mathbf{h}}\,\overleftrightarrow{A}\,\mathbf{h}$, $\sigma = \tilde{\mathbf{h}}\,\overleftrightarrow{\sigma}\,\mathbf{h}$. Here, $\mathbf{h}$ is a direction cosine of the magnetic field.

We measured the temperature dependence of δ at several angles. From their slopes, we determined A and σ for those angles shown in Table I and determined the following hyperfine-coupling tensors and chemical-shift tensor:

$$\begin{pmatrix} A_{aa} & A_{ab'} & A_{ac^*} \\ A_{b'a} & A_{b'b'} & A_{b'c^*} \\ A_{c^*a} & A_{c^*b'} & A_{c^*c^*} \end{pmatrix}_H = \begin{pmatrix} 9.0(4) & 0.0(1) & 0.3(2) \\ 0.0(1) & 1.08(8) & 0.21(7) \\ 0.3(2) & 0.21(7) & 1.42(4) \end{pmatrix} \times (\mathrm{kOe}/\mu_B), \quad (1)$$

$$\begin{pmatrix} A_{aa} & A_{ab'} & A_{ac^*} \\ A_{b'a} & A_{b'b'} & A_{b'c^*} \\ A_{c^*a} & A_{c^*b'} & A_{c^*c^*} \end{pmatrix}_L = \begin{pmatrix} 5.0(2) & 0.1(2) & 0.4(3) \\ 0.1(2) & -0.46(7) & 0.27(5) \\ 0.4(3) & 0.27(5) & 0.08(4) \end{pmatrix} \times (\mathrm{kOe}/\mu_B), \quad (2)$$

$$\begin{pmatrix} \sigma_{aa} & \sigma_{ab'} & \sigma_{ac^*} \\ \sigma_{b'a} & \sigma_{b'b'} & \sigma_{b'c^*} \\ \sigma_{c^*a} & \sigma_{c^*b'} & \sigma_{c^*c^*} \end{pmatrix} = \begin{pmatrix} -0.8(1) & 0.0(1) & -0.2(1) \\ 0.0(1) & 1.176(1) & -0.301(1) \\ -0.2(1) & -0.301(1) & 0.8243(6) \end{pmatrix} \times (10^2\ \mathrm{ppm}). \quad (3)$$

Because $(TMTSF)_2X$ salts display the same isomorphism, we can use the hyperfine-coupling tensor as the basic parameter for the ^{13}C-NMR of $(TMTSF)_2X$. As mentioned in a later section, for the discussion of electronic correlations evaluated by NMR, the ratio $(A_\perp/\sqrt{2}A_\parallel)^2 \simeq (A_{aa}^2 + A_{c^*c^*}^2 + 2A_{ac^*}A_{c^*a})/2A_{b'b'}^2$ of matrix elements in the hyperfine-coupling tensor is needed.

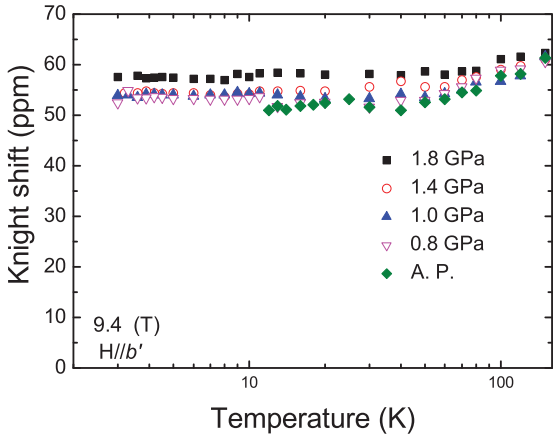

FIG. 4. (Color online) Temperature dependence of the Knight shift.

B. Knight shift and FL behavior

Because the HFCC of L was very small, we focused on the pressure dependence at the H site. We evaluated K at ambient pressure and under other pressures by subtracting σ from δ as in Fig. 4. At 150 K, K of H has almost the same value of 62 ppm at all pressures, whereas in ^{77}Se-NMR, χ_s, which was evaluated from $(T_1T)^{-1}$, decreased with the application of pressure.[20] Under ambient pressure, the uniform spin susceptibility, which corresponds to K, slightly decreases with decreasing temperature. Various explanations exist for this decrease at low temperatures, such as the dimensionality of the salt, electron correlation, and thermal expansion.[20] The decrease at low temperatures was suppressed by applying pressure, and the uniform spin susceptibility was almost constant at 1.8 GPa, suggesting characteristic FL behavior.

C. T_1 and magnetic fluctuations

The main purpose of our study is to assess magnetic fluctuations under pressures greater than ∼1 GPa. The behavior of the salt in this pressure region suggests a correlation between NFL behavior and magnetic fluctuations.

Figure 5 shows the temperature dependence of $(T_1T)^{-1}$ at ambient and other pressures. Similar to the NMR spectra, all relaxation profiles are fitted by a single exponential function without spatial inhomogeneities (as shown in Fig. 6). The increase in $(T_1T)^{-1}$ at ambient pressure and low temperatures, which was suppressed by increasing the pressure, indicates the development of antiferromagnetic SDW fluctuation. This behavior is consistent with that of the previous ^{77}Se-NMR below ∼1 GPa.[10,20] Finally, $(T_1T)^{-1}$ becomes almost temperature independent at 1.8 GPa. Generally, $(T_1T)^{-1}$ is expressed by the following formula in anisotropic coupling:[21,22]

$$\frac{1}{T_1T} = \frac{2\gamma_n^2 k_{\rm B}}{(\gamma_e\hbar)^2} \Sigma_{\boldsymbol{q}} F a_{\boldsymbol{q}} a_{-\boldsymbol{q}} \frac{\chi_\perp''(\boldsymbol{q},\omega_0)}{\omega_0}. \quad (4)$$

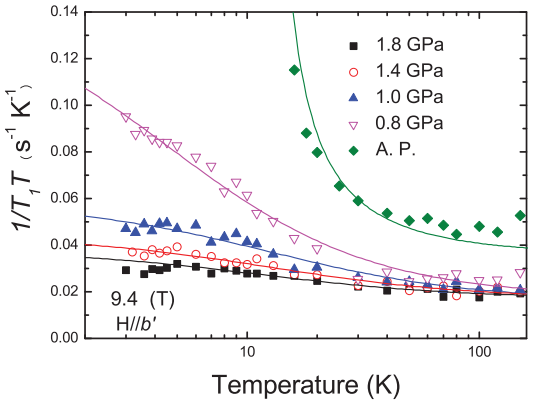

FIG. 5. (Color online) Temperature dependence of $(T_1T)^{-1}$ at ambient and other pressures.

Here, γ_n, γ_e, k_B, and $\hbar$ are the gyromagnetic ratio of the nucleus and electrons, the Boltzmann constant, and the Planck constant, respectively. The constants $a_{\boldsymbol{q}}$ and F are the isotropic HFCC and the form factor in the anisotropic coupling system. The imaginary part of the dynamic spin susceptibility vertical to the quantization axis is $\chi''_{\perp}$, ω_0 is the NMR frequency, and variable $\boldsymbol{q}$ is the vector of a staggered magnetization. In FL, $(T_1T)^{-1}$ is proportional to the square of the uniform spin susceptibility and is temperature independent. The rate $(T_1T)^{-1}$ detects all staggered magnetic fluctuations with the wave-number vector $\boldsymbol{q}$. Hence, to distinguish the fluctuations in $\boldsymbol{q} = \boldsymbol{Q}_{\rm SDW}$ from the temperature dependence of $(T_1T)^{-1}$ we measured this rate over a wide temperature range.[20] In the vicinity of the SDW phase transition, the summation term is divided into the terms of $\boldsymbol{q} = \boldsymbol{Q}_{\rm SDW}$ and $\boldsymbol{q} \neq \boldsymbol{Q}_{\rm SDW}$, i.e.,

$$(T_1T)^{-1} = (T_1T)^{-1}_{\rm SDW} + (T_1T)^{-1}_0. \tag{5}$$

Magnetic fluctuations of $\boldsymbol{q} \neq \boldsymbol{Q}_{\rm SDW}$, i.e., $(T_1T)^{-1}_0$, can be expressed in the following formula by using the Korringa enhancement factor $\mathcal{K}$:

$$\frac{1}{(T_1T)_0K^2} = \left(\frac{A_\perp}{\sqrt{2}A_\parallel}\right)^2 \frac{4\pi k_B}{\hbar}\left(\frac{\gamma_n}{\gamma_e}\right)^2 \mathcal{K}. \tag{6}$$

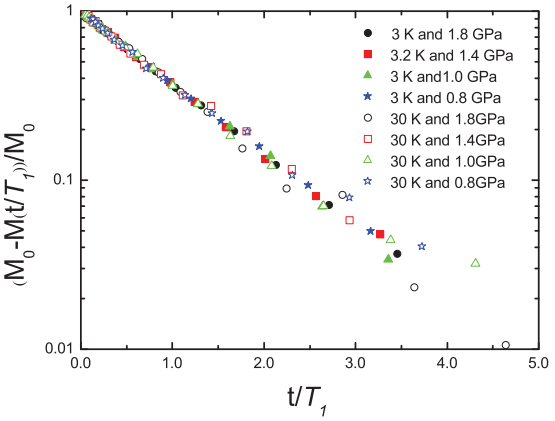

FIG. 6. (Color online) Relaxation profiles at various temperatures and pressures.

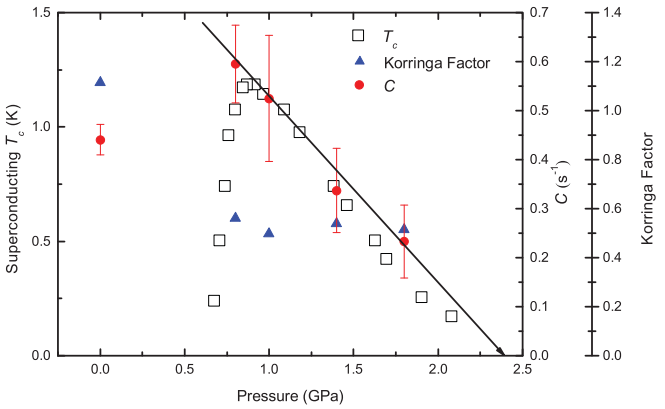

FIG. 7. (Color online) Pressure dependence of T_c, C, and the Korringa factor $\mathcal{K}$[5].

Here, $(A_\perp/\sqrt{2}A_\parallel)^2$ is a form factor estimated to be ∼36 by using the hyperfine-coupling tensor, which is evaluated using the angle dependence ^{13}C-NMR at ambient pressure. When $\mathcal{K} = 1$, the system is regarded as a simple metal; when $\mathcal{K} > 1$, an antiferromagnetic contribution is expected; and when $\mathcal{K} < 1$, a ferromagnetic contribution is expected. We fitted the temperature dependence of $(T_1T)^{-1}$ by using a Curie-Weiss expression $(T_1T)^{-1} = C/(T + \Theta) + (T_1T)^{-1}_0$ (Ref. 20) at each pressure with $\Theta = -11.5$ K at ambient pressure, $\Theta = 4.6$ K at 0.8 GPa, $\Theta = 12.5$ K at 1.0 GPa, $\Theta = 12.6$ K at 1.4 GPa, and $\Theta = 11.3$ K at 1.8 GPa, whereas $(T_1T)^{-1}$ in ^{77}Se-NMR on $(TMTSF)_2ClO_4$ was fitted by using $(T_1T)^{-1} = C/(T + \Theta)$ at low temperatures.[23] The value of Θ at 0.8 GPa is consistent with $\Theta \sim 2$ K in $(TMTSF)_2ClO_4$ salt. We evaluated the pressure dependence of $\mathcal{K}$ from the value of K at 150 K at which a contribution of $(T_1T)^{-1}_{\rm SDW}$ was negligible. We show the pressure dependence of C and $\mathcal{K}$ with T_c in Fig. 7. The decrease of $(T_1T)^{-1}$ from ambient pressure to ∼1 GPa in ^{77}Se and ^{13}C-NMR were not because of the decrease in the uniform spin susceptibility but because of the decrease in $\mathcal{K}$. $\mathcal{K}$ significantly varies as the pressure changes from ambient pressure to 0.8 GPa. This result is considered to imply increase in the dimensionality. Whereas T_c decreased above ∼1 GPa, $\mathcal{K}$ was almost constant above ∼1 GPa; the value of $\mathcal{K} \sim 0.55$ suggested that the electron correlation with $\boldsymbol{q} \neq \boldsymbol{Q}_{\rm SDW}$ exhibits weakness as with the simple alkali metals[24] and is not connected with NFL behavior and T_c. In contrast, C decreased to nearly zero with the increasing pressure at which the resistivity corresponded to that of the FL state (T^2 dependence), and T_c decreased to zero. These results suggest that the electron system changed from NFL to FL in response to the reduction in the antiferromagnetic SDW fluctuation with increasing pressure. Hence, the origin of NFL behavior is expected because of the SDW fluctuation. Considering the connection between the emergence of FL behavior and the disappearance of superconductivity, the SDW fluctuation is connected to the mechanism of superconductivity in $(TMTSF)_2PF_6$.

We also observed similar behavior in a two-dimensional organic superconductor. The organic conductor κ-$(BEDT\text{-}TTF)_2Hg_{2.87}Br_8$ exhibits bulk superconductivity above 0.4 GPa.[25] Although κ-$(BEDT\text{-}TTF)_2Hg_{2.87}Br_8$ and

$(TMTSF)_2PF_6$ differ in crystal structures and dimensionalities, the adjacency of the superconducting phase and the antiferromagnetic phase, and the connection between T_c and NFL behaviors, which was observed in the electric resistivity,[25] were suggested. In κ-$(BEDT\text{-}TTF)_2Hg_{2.87}Br_8$, NMR measurements suggest that the origin of the change of the electron system from NFL to FL was because of a reduction in antiferromagnetic fluctuations.[26]

IV. SUMMARY

In summary, we performed ^{13}C-NMR measurements on $(TMTSF)_2PF_6$ in order to investigate the connection between NFL behavior, which was observed by resistivity measurement, and magnetism. We were able to evaluate $(T_1T)^{-1}$ and the Knight shift corresponding to the uniform spin susceptibility under pressures up to 1.8 GPa. The temperature dependence of $(T_1T)^{-1}$ exhibited large antiferromagnetic fluctuations at ambient pressure. When pressure increased, the development of antiferromagnetic fluctuations was suppressed, and $(T_1T)^{-1}$ and the Knight shift were almost constant at 1.8 GPa, suggesting the electron system reached FL state at 1.8 GPa. The analysis of $(T_1T)^{-1}$ implies that the origin of NFL behavior was the SDW fluctuation. The connection between the emergence of FL behavior and the disappearance of superconductivity suggests that the SDW fluctuation relates to the superconductivity in $(TMTSF)_2PF_6$.

ACKNOWLEDGMENTS

The authors thank N. Matsunaga and K. Nomura of Hokkaido University for the high-pressure measurement. This study was supported in part by a Grant-in-Aid for Science Research (Grant No. 18540306) from the Ministry of Education, Culture, Sports, Science and Technology.

*atkawa@phys.sci.hokudai.ac.jp

[1] R. H. McKenzie, Science **278**, 820 (1997).
[2] K. Bechgaard, C. S. Jacobsen, K. Mortensen, H. J. Pedersen, and N. Thorup, Solid State Commun. **33**, 1119 (1980).
[3] N. Thorup, G. Rindorf, and H. Soling, Acta Crystallogr. Sect. B **37**, 1236 (1981).
[4] D. Jérome, Science **252**, 1509 (1991).
[5] N. Doiron-Leyraud, P. Auban-Senzier, S. Renede Cotret, C. Bourbonnais, D. Jérome, K. Bechgaard, and L. Taillefer, Phys. Rev. B **80**, 214531 (2009).
[6] J. C. Nickel, R. Duprat, C. Bourbonnais, and N. Dupuis, Phys. Rev. B **73**, 165126 (2006).
[7] C. Bourbonnais and A. Sedeki, Phys. Rev. B **80**, 085105 (2009).
[8] I. J. Lee, S. E. Brown, W. Yu, M. J. Naughton, and P. M. Chaikin, Phys. Rev. Lett. **94**, 197001 (2005).
[9] I. J. Lee, D. S. Chow, W. G. Clark, M. J. Strouse, M. J. Naughton, P. M. Chaikin, and S. E. Brown, Phys. Rev. B **68**, 092510 (2003).
[10] F. Creuzet, C. Bourbonnais, L. G. Caron, D. Jérome, and A. Moradpour, Synth. Met. **19**, 277 (1987).
[11] G. E. Pake, J. Chem. Phys. **16**, 327 (1948).
[12] E. Barthel, G. Quirion, P. Wzietek, D. Jérome, J. B. Christensen, M. Jørgensen, and K. Bechgaard, Europhys. Lett. **21**, 87 (1993).
[13] K. Bechgaard, D. O. Cowan, and A. N. Bloch, J. Chem. Soc. Chem. Commun. **22**, 937 (1974).
[14] A. Moradpour, V. Peyrussan, I. Johansen, and K. Bechgaard, J. Org. Chem. **48**, 388 (1983).
[15] J. Yamada, S. Satoki, S. Mishima, N. Akashi, K. Tkakahashi, N. Masuda, Y. Nishimoto, S. Takahashi, and H. Anzai, J. Org. Chem. **61**, 3987 (1996).
[16] W. Kang, S. T. Hannahs, and P. M. Chaikin, Phys. Rev. Lett. **70**, 3091 (1993).
[17] K. Miyagawa, A. Kawamoto, and K. Kanoda, Phys. Rev. B **62**, R7679 (2000).
[18] S. Moroto, K. I. Hiraki, Y. Takano, Y. Kubo, T. Takahashi, H. M. Yamamot, and T. Nakamura, J. Phys. IV (France) **114**, 339 (2004).
[19] J. C. Scott, H. J. Pedersen, and K. Bechgaard, Phys. Rev. Lett. **45**, 2125 (1980).
[20] P. Wzietek, F. Creuzet, C. Bourbonnais, D. Jérome, K. Bechgaard, and P. Batail, J. Phys. I (France) **3**, 171 (1993).
[21] A. Kawamoto, K. Miyagawa, Y. Nakazawa, and K. Kanoda, Phys. Rev. B **52**, 15522 (1995).
[22] T. Moriya, J. Phys. Soc. Jpn. **18**, 516 (1962).
[23] J. Shinagawa, Y. Kurosaki, F. Zhang, C. Parker, S. E. Brown, D. Jérome, K. Bechgaard, and J. B. Christensen, Phys. Rev. Lett. **98**, 147002 (2007).
[24] G. C. Carter, L. H. Benett, and D. J. Kahn, *Metallic Shifts in NMR, Part I* (New York, 1977).
[25] H. Taniguchi, T. Okuhara, T. Nagani, K. Satoh, N. Môri, Y. Shimizu, M. Hedo, and Y. Uwatoko, J. Phys. Soc. Jpn. **76**, 113709 (2007).
[26] Y. Eto, M. Itaya, and A. Kawamoto, Phys. Rev. B **81**, 212503 (2010).